ZANCO Journal of Pure and Applied Sciences

TYPE Original article
DOI http://dx.doi.org/10.21271/ZJPAS.37.6.12

OPEN ACCESS

*Corresponding author

Skala Hassan Hussen

skala.hussen@su.edu.krd

RECEIVED :14 /04 /2025
ACCEPTED :12/07/ 2025
PUBLISHED :31/ 12/ 2025

KEYWORDS:

Leukemia, Image preprocessing, Classification, Transfer learning, Deep learning.

A Comparative Evaluation of Transfer Learning Techniques for White Blood Cell Detection

Skala Hassan Hussen[1], Shahab Wahab Kareem[2&3]

1Department of Software Engineering & Informatics, College of Engineering, Salahaddin University - Erbil, Erbil, Kurdistan Region, Iraq.
2Technical Information System Engineering Dept., Erbil Technical Engineering College, Erbil Polytechnic University,
3Department of Computer Technical Engineering, Al-Qalam University College, Kirkuk, Iraq.

ABSTRACT

Standard deep-learning (DL) and machine learning (ML) approaches are valuable frameworks in computer vision that improve the accuracy of medical image diagnosis and classification, including the identification of microscopic blood cells. This study examines the detection and categorization of acute leukemia in detail. Improving patient prognosis and treatment options requires early diagnosis, categorization, and accurate detection of white blood cells. Developing a precise and effective model for identifying and classifying malignancies in white blood cell (WBC) images remains challenging despite the widespread use of microscopes for blood cell examination and advancements in AI-based detection techniques. To address these challenges, the authors utilized a total of 48,000 images, comprising both public and private sources, after augmenting three classes of white blood cell (WBC) cells. This study aims to evaluate whether Vision Transformers can match or surpass the performance of convolutional neural networks (CNNs) for WBC classification using large-scale datasets, and to determine whether spatial inductive biases inherent in CNNs offer a measurable advantage, and achieved accuracies of 95.07%, 95.27%, 82.66%, 92.00%, and 83.59%., also creating an Ensemble model that combine three models(VGG19, Xception, and U-Net) running on gpu.v2-4090x4 server with RAM 384 GB because of volume of data which achieving accuracy of 92%, Also study proposed an architecture for deep learning that automatically recognizes and classifies WBC images, categorizing them into five types. The models for detection and classification techniques were also assessed using accuracy, F1 score, recall, and precision for each class of WBC.

List of Illustrations of Abbreviations

DL	Deep Learning
WBC	White Blood Cell
Vit	Vision Transformer
MIA	Medical image analysis
ML	Machine Learning
VGG	Visual Geometry Group
RBC	Red Blood Cell
PBC	Platelet Blood Cell

1.Introduction

The human immune system relies on leukocytes to identify and eliminate pathogens, including viruses, bacteria, and malignant cells. White blood cell classification is essential for accurately diagnosing and treating various illnesses and medical disorders. Medical image analysis (MIA) utilizes machine learning techniques to support physicians in making informed decisions within healthcare systems. Different imaging modalities detect malaria, leukemia, anemia, lung cancer, and brain tumors.(Asghar et al., 2024a). The types of blood cells are platelets, red blood cells, and white blood cells, also known as leukocytes. Traditional (ML) and deep learning (DL) techniques have improved the classification of white blood cells (WBC) and the segmentation of white blood cells in blood smear images. The three main kinds of blood cells are red blood cells, white blood cells (leukocytes), and platelets.(Asgari Taghanaki *et al.*, 2021). Traditional machine learning and deep learning techniques have improved white blood cell segmentation in blood smear images. (Asghar *et al.*, 2024b). Red blood cells, white blood cells, and platelet parameters are evaluated during the test. Automatic blood analyzers from different vendors can assess a wide range of characteristics. The WBC count displays the precise amount or proportion of B, N, M, L, and E. Granulocytes and agranulocytes are two categories into which the kinds of white blood cells (WBCs) can be segmented.

As shown in Figure 1, each type of white blood cell (WBC) has a distinct role; variations in each cell type indicate the patient's pathological condition. Blood analyzers produce the WBC differential count results based on concepts related to granularity, size, biochemical characteristics, and other factors.(Dai *et al.*, 2020). Nevertheless, examining blood by Proficient and experienced medical technologists is essential. Conventional techniques for blood analysis, used to enumerate white blood cells, may lack precision and efficiency, with the proficiency of laboratory staff significantly influencing the test's reliability. A critical study methodology for image categorization to attain enhanced and precise outcomes. Deep learning methodologies like those presented in this study are employed across several medical applications. The percentage of WBC through each class is shown in Figure 2. The study noticed that the rate of neutrophils is the highest, while basophils have the lowest percentage in the blood.

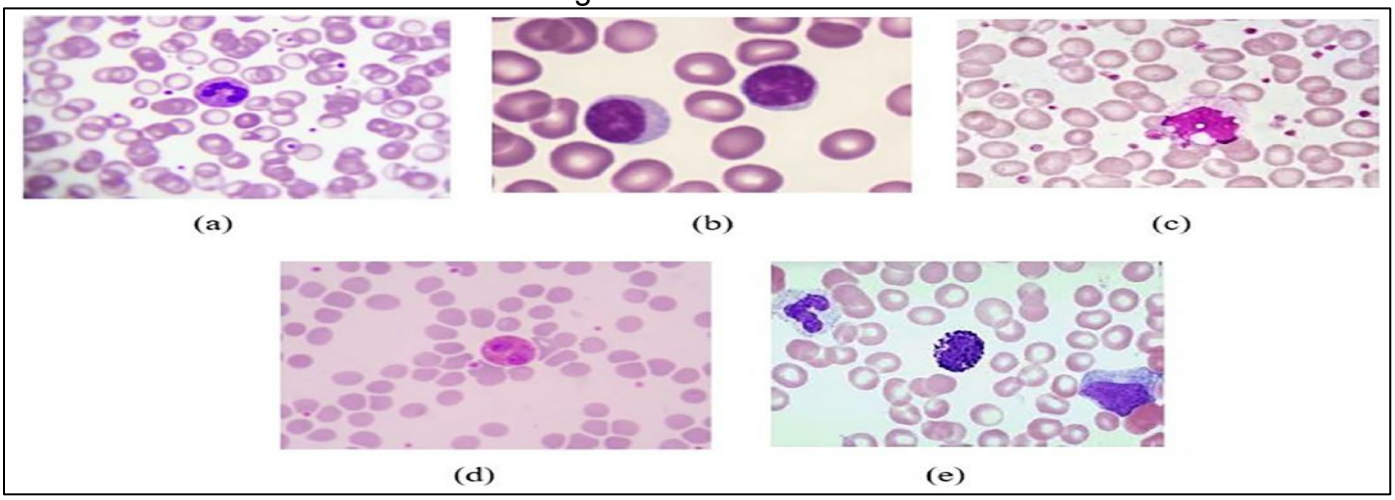

Figure 1 White blood cell types include lymphocytes, monocytes, eosinophils, neutrophils, and basophils. (Asghar *et al.*, 2024c)

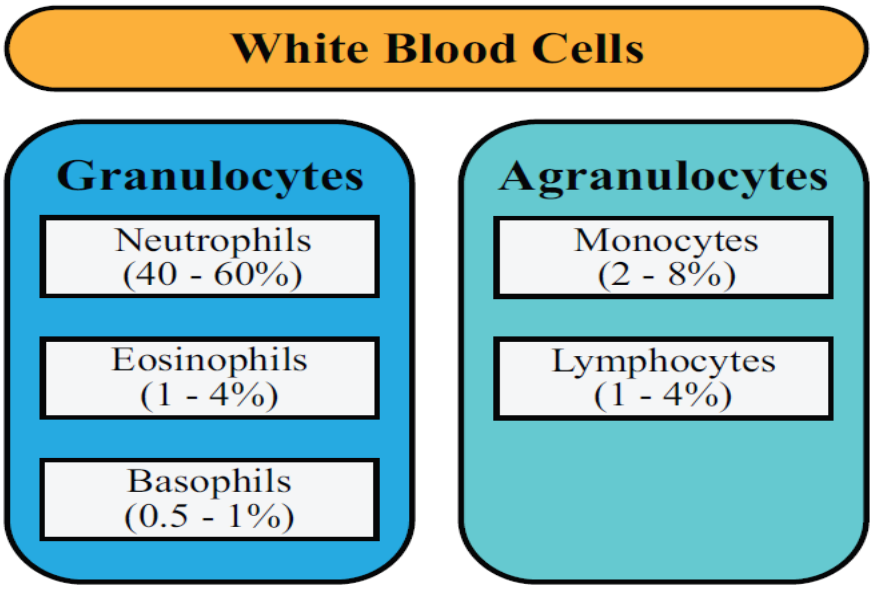

Figure 2: Classification of Leukocytes.*(Tamang, Baral and Paing, 2022)*

A 2012 study indicated that approximately 352,000 people and children globally are diagnosed with leukaemia, a condition originating in the bone marrow and characterized by aberrant proliferation of WBC. Machine learning and image processing methods are utilized in many conventional computer-aided systems. Pre-processing, segmentation, feature extraction, and classification are just a few of the procedures that are commonly included in these methods. Each step's efficacy is contingent upon the completion of the preceding stage. The efficacy of classification depends on the effectiveness of previous feature extraction. This is contingent upon the efficacy of the segmentation that came before. Consequently, achieving high classification accuracy necessitates successfully executing all phases (Loey, Naman, and Zayed, 2020a). Deep learning (DL) has made an important. Therefore, we use transfer learning, which involves adapting a successful deep network created for one problem to solve another rather than starting from scratch when building a deep neural network. Additionally, some algorithms, such as Vision Transformer (ViT), used for NLP, and U-Net, used for segmentation, make it challenging to perform classification. Additionally, another challenge is Computational Complexity. The authors aimed to utilize transfer learning models in big data for white blood cell images and make a comparative evaluation between them. However, constructing and training deep neural networks is a challenging and time-consuming process. Consequently, some challenges exist with this model, including the handling of a low number of basophil cells during data collection. In contrast, this paper utilizes the classification of WBC to enable the model to generalize across other datasets and determine the optimal architecture. This is accomplished in this research by evaluating and improving five deep learning models from a large and diverse data source.

The study contribution presented in this work is to utilize a transfer learning model that has not been previously applied to big data for the classification of White Blood Cells, and additionally, to employ the U-Net model for classification rather than segmentation models. As well as utilizing an Ensemble model to combine three models, VGG19, U-Net, and Xception. The rest of the paper is structured as follows: in section 1, provide an overview of White Blood Cells with problems and contributions, in section 2. Review the recent

study on the classification and segmentation of white blood cells. in Section 3. Section 4 explains the experimental data, dataset description, training setups, performance metrics, and comparisons with previous approaches. It also studies relationship outcomes, model assumptions, and recommendations for improving the model. In Section 5, this paper concludes by reviewing its contributions and outlining future research directions.

2.Related work

The classification and detection of "white blood cell" cancer, which has developed globally from 2018 to 2024, was the aim of the study. This study aims to evaluate the most prevalent methods for detecting and classifying WBC cancer that are globally available. (Sahlol, Kollmannsberger and Ewees, 2020a) Proposed a technique for detecting leukemic white blood cells. Features of the white blood cells were retrieved using a VGG-19 model, and the Statically Enhanced Slap Swarm Algorithm (SESSA) was first used to extract features. SVM, or support vector machines, were used in the classification stage. A dataset comprising 260 images was used to evaluate the model, yielding a classification accuracy of 96.11%. The ALL-IDB2 and C-NMC databases were used to test the model and related techniques, which were then compared. Developed two automated classification techniques for distinguishing between normal and pathological microscopic blood cells. (Loey, Naman and Zayed, 2020b) Image preprocessing involves translating, reflecting, and rotating images. The initial approach, AlexNet, was utilized for feature extraction and classification, as well as integrated linear discriminants (LDS), and K-NN stands for K-nearest neighbors.

The second approach involved classifying and extracting features using the AlexNet model. A total of 2,820 images were used to evaluate the two methods. The first method's average accuracy was 98.69%, whereas the accuracy of the second method was 100%. The study sought to compare the performance metrics of deep learning and traditional methodologies for diagnosing and categorizing acute leukemia. LeukNet, an engineered convolutional neural network, achieved a classification accuracy of 98.20% in identifying leukemia using 3,536 WBC images (Vogado et al., 2018). A pre-trained AlexNet was used to categorize ALL and its subtypes using the 260-picture ALL-IDB2 dataset, with an average categorization accuracy of 96.06% (Shafique and Tehsin, 2018). The study focusses on WBC classification as discussed by Sahlol, Kollmannsberger, and Ewees (2020b). The study improves CNNs by incorporating the Salp Swarm technique on the ALL-IDB2 dataset. It utilizes a VGG network and SESSA to extract feature vectors and retain only the pertinent ones.

A dataset of 10,295 cellulars was utilized. CNN achieved an accuracy of 98.4%, whereas SVM attained an accuracy of 90.6% (Khalid Altarawneh, 2023). The study analyzed white blood cells. (ELEN and TURAN, 2019a) Initially, statistical and geometric characteristics are derived from microscopic blood images. Subsequently, the efficacy of the classifications is assessed using a decision tree (DT), k-NN (k-nearest neighbour), and multinomial logistic regression. Ansari et al. developed a deep-learning model using multiple linear regression, naïve Bayes, random forest, and SVM techniques to recognize acute leukemia from images of monocytes and lymphocytes. The model, which used a Generative Adversarial Network (GAN), achieved an accuracy rating of 99.5%. (Ansari et al., 2023). A combined model that uses CNN and recurrent neural networks was used to sort 12,444 images, reaching a success rate of 90.79% compared to just using CNN (ELEN and TURAN, 2019a) and introduced a two-step deep learning model for identifying immature white blood cells and abnormal lymphocytes. The problem is the unequal distribution of white blood cells in the bloodstream.

A new approach called the "GTDCAE WBC augmentation model," which mixes geometric transformation (GT) and a deep convolutional autoencoder (DCAE), was used to analyse the samples. The "two-stage DCAE-CNN atypical WBC classification model," a hybrid multiclassification model, classifies atypical WBCs into eight distinct classes. The model's average precision, sensitivity, and accuracy were 98%, 97%, and 97%, respectively (Elhassan et al., 2023). The two-stage DCAE-CNN atypical WBC

classification model, which is a hybrid multiclassification model, accurately sorts atypical WBCs into eight categories with 97% accuracy, 96% sensitivity, and 98% precision. Ahmad et al. (2023) introduced an enhanced hybrid approach for optimal deep feature extraction with DenseNet201 and Darknet53. Singh et al. (2023) used CNN and optimizers such as SGD, Adadelta, and Adam to classify white blood cells with 97% accuracy, 98% recall, and a 98% F1 score. (Darrin et al., 2023) presented an analysis method for video containing automatically categorizing red blood cells (RBC) that are out of balance to track the health of sickle cell anemia patients.

The videos ranged from 6 to 100 frames. The integration of a recurrent CNN with a convolutional neural network (CNN) model yielded an accuracy of 96% and an F1 score of 0.95. To solve the problem of the classification of blood cells. As shown in the sections, there are very accurate methods using CNN, like LeukNet and AlexNet models, but they might not work well with different datasets or might not fix the issue of uneven class distribution. This research builds on previous studies by using data enhancement and adjusting models across five main designs, using a large database created by combining three different collections. (Kumar et al., 2020) The SN-AM dataset classified multiple myeloma and acute lymphoblastic leukemia with 97.2% accuracy. Using You Only Look Using YOLOv5, Luong et al. showed a way to identify, sort, and count blood cells, helping to tell leukaemia cells apart from normal white blood cells. (Luong et al., 2022) Use YOLOv5 to detect, categorize, and count blood cells to distinguish leukemia cells from normal white blood cells.

Zou et al. (2025) used MobileNetV2 to develop a light and effective WBC classification model, which had multiscale feature extraction and an attention mechanism added. Their scheme lies between achieving a great deal of accuracy and minimal computation expense, such that it is suitable in a real-time setting or somewhere that is result-constrained. Duc et al. (2025) proposed a new architecture with multi-hop attention-based graph neural networks (GNNs) to categorise WBCs. They were able to grasp a much better understanding and reliability to provide different cell types of classification based on modeling spatial and relational dependencies between the structures of cells. The comparative analysis of the automated UIMD PBIA cell analyzer performance by Kim et al. (2025) consisted of the evaluation against the commercial Sysmex DI-60. Similar results in accuracy were presented in the UIMD PBIA system, providing a plausible solution to implement automation of clinical WBC classification. Sutabri and Putra (2025) applied a hybrid method of SMOTE-SVM, fusion of the features and segmentation by using the Gaussian Mixture Model (GMM). This technique was able to enhance the process of characterizing imbalanced WBC datasets and better cell segmentation in an unsupervised way. Table 1 presents pertinent review papers, their details, and key points.

After reviewing and comparing the study with previous research, the author noticed that most existing studies used relatively small datasets, yet they still achieved good accuracy. What makes this study different is that it used a much larger, big dataset that better reflects real-world conditions. Also, many of those studies applied the U-Net model mainly for white blood cell segmentation. In contrast, the study used U-Net differently for classification, which is less common. Moreover, applied this deep learning model on a big dataset, something that, to the best of knowledge, hasn’t been widely done yet. This makes the approach both unique and forward-looking in the field.

Table 1: Relevant Research on White Blood Cell Detection Diagnosis.

References	Algorithm	Datasets	Contribution & results	limitations
(Prayitno *et al.*, 2021)	They proposed a quantitative estimator named Attack Effect on Parameter (AEP). To make robustness FL.	MNIST and CIFAR-10	Additionally, they lowered the learning rate (Lr) to 0.01 and used the SGD optimizer; the findings demonstrate that, in our experimental setup, only CMA can lessen the attack effect. By using FL-WBC in addition to CMA.	Not WBC-specific; lacks clinical applicability and medical dataset testing.
(Crimi and Bakas, 2022)	They used ViT for WBC detection.	Utilized Kaggle, and Rabin-WBC dataset	The ViT model trained for binary classification achieved 99.70% accuracy, 99.54% recall, 99.32% precision, and a 99.43% F-1 score during the testing phase.	Only binary classification; no testing on full multiclass spectrum; limited generalizability.
(Chen *et al.*, 2024)	Most deep learning methods for WBC classification struggle to detect minor structural differences; however, combining low-level details with high-level features improves their performance.	OTSU, an adaptive threshold segmentation technique, separated the dataset's WBCs from the background based on grayscale differences.	accuracy of 80.3%,	Relatively low accuracy; segmentation-focused method adapted for classification.
(Jung *et al.*, 2019)	W-Net, a CNN-based technique for WBC categorization, is proposed in this paper.	Korean Catholic University, which has 6,562 real images	W-Net achieves 97%.	Limited dataset; lacks transformer or ensemble comparison.
(Nguyen *et al.*, 2021)	The inception module, depth-wise squeeze-and-excitation block (DSEB), and pyramid pooling module (PPM) are crucial components in the construction and operation of many electronic devices.	Rabin, AML, PBC, and LDWBC	an accuracy of over 94%,	The complex model structure has not been benchmarked against ViT or real-time performance.
(Gu *et al.*, 2024)	The integration of the pre-trained InceptionV3 model with transfer learning techniques	Leukemia Image Database (ALL-IDB).	Accuracy over 96%,	Small dataset; lacks generalized multiclass capability.
(Fang, Di and Cao, 2024)	Super Resolution Generative Adversarial Network (SRGAN) and Visual Geometry Group 19 (VGG19)	(BCCD) dataset, which includes 12,447	accuracy of 94.87 %,	Focus on preprocessing rather than classifier robustness or generalization.
(Jung *et al.*, 2021)	A comprehensive dataset consist 6,562	A dataset of 6,562 images is	W-Net accomplishes of 97%.	Relatively small dataset; no

	authentic images of five WBC types is utilized to evaluate the CNN-based W-Net methodology.	available from (CUK)the Catholic University of Korea .		transformer comparison; does not address class imbalance.
(Saidani *et al.*, 2024)	traditional deep learning and transfer learning models include ResNet50, Mobile-NetV2, InceptionV3, and VGG16.	The dataset is from the Dataport's IEEE the dataset comprises 3539 images, four classes utilized	MobileNetV2 obtained an accuracy value of 0.7847, InceptionV3 secured a value of 0.9720, and VGG 16 secured a score of 0.9609.	Moderate dataset size; lacks transformer-based models; unclear data augmentation strategy.
(Sun *et al.*, no date)	Support vector machines (SVM) and U-Net	The BCCD, LISC, and Rabin-WBC datasets	accuracy of 99.45%, 97.62%, and 96.81%,	No comparative evaluation of CNN vs Transformer; limited focus on generalizability to other datasets.
(Şengür *et al.*, 2019a)	This is used Google Vit and ImageNet CNN	Using the PBC dataset and the BCCD dataset. 4 classes utilized	Overall, 86% of deep features are classified correctly.	Low performance; lacks robust multiclass validation; no ensemble or augmentation techniques.
(Şengür *et al.*, 2019b)	An LSTM network is employed for categorization. When extracting color features.	From the Kaggle 4 classes utilized	achieve 85.7% accuracy	Color-based features are fragile to lighting variation; lacks deep model validation.
(Jung *et al.*, 2022)	W-Net is a CNN-based method for WBC classification.	The collection includes 6562 real-world images from the Catholic University of Korea (CUK).	With dice similarity of 98.9 and 91.6%	Dice score used rather than classification metrics; lacks ViT comparison.
(Qin, Hong and Tang, 2018)	Using deep learning-CNN	Image provides from three places Nanjing, University Medical, and School's Drum Tower Hospital	The outcome demonstrates that our CNN model completed the classification assignment with an accuracy of roughly 88.5%.	No state-of-the-art comparison; lacks focus on diverse cell types.
(Gupta *et al.*, 2019)	Random Forest, KNN, Decision Tree, and Logistic Regression are all integrated into the suggested Binary Bat feature selection method (OBBA).	OBBA is utilized on the White Blood Cells dataset	97.91% 97.91% 97.91% 95.83%	Not deep learning; cannot capture complex visual features like CNNs or ViT.
(Othman,	The Back Propagation	N/A	For the WBC types of	Simple network;

Mohammed and Ali, 2017)	(BP) algorithm-trained MLP		neutrophils, lymphocytes, and basophils, classification accuracy is 100%, whereas 91% Accuracy has been achieved for the other two categories.	lacks scalability for large datasets or high-resolution images.
(Derdour, Ahmim and Benjedou, 2019)	Support vector machines (SVM).	Tested on Twenty-seven authentic microscopic color images	accuracy reaching 95%.	Extremely small sample size; not scalable or reliable for clinical use.
(ELEN and TURAN, 2019b)	Multinomial Logistic Regression (MLR) algorithm	350 (WBC) images were used to create 500 bits of data.	95% test	Outdated technique; lacks modern CNN or DL model benchmarking.
(Prinyakupt and Pluempitiwiriyawej, 2015)	Bayes classifiers that are naïve and linear.	(dataset 1)Tested 555 images under a light microscope. (dataset 2): CellaVision Competency software had 477 images	Both methods have an accuracy of over 90%	Lacks deep learning comparison; older datasets and methodology.
(Hawezi, Khoshaba and Kareem, 2022)	Zero-R, random forest, random tree, model tree classifier (M5P), and support vector machine with regression (SMOreg).	No dataset is mentioned here.	The outcome demonstrated that, for the input dataset, Random Forest is the most effective algorithm among the ones mentioned above. it is 94%	No visual feature learning; not adapted to image-based medical data.

3.Methodology

This organized pipeline approach is used in the deep learning-based image categorization project. Data collection is the first step, which involves gathering a dataset to use as the basis for evaluation and training. After being gathered, images are pre-processed to enhance quality, reduce noise, and ensure uniformity. The images are resized to a consistent size after preprocessing to ensure compatibility with deep-learning models. Data augmentation methods, including rotation, flipping, and brightness adjustments, enhance the dataset's diversity and improve model generalization. After completing these preparation stages, the performance of several deep learning models is compared through training and evaluation. Specifically, the presented study aims to develop an overall deep learning approach to white blood cell classification using transfer learning and hyperparameter optimization across two main categories and architectures (U-Net, Xception, VGG19, ResNet50, Vision Transformer) and a large-scale dataset of 48,000 images. This methodology ensures a systematic approach to model evaluation and data preparation, yielding a robust classification system based on deep learning. As shown in the diagram below. As noted in the previous study, the dataset used in an earlier paper is not as large, as it consists of fewer than three datasets. In contrast, we collect big data and employ a transfer learning model.

3.1. **Dataset**

The proposed WBC classification approach utilizes a Blood Cell Classification dataset comprising five categories: Eosinophil, Monocyte, Lymphocyte, Basophil, and Neutrophil images. The author used 48,000 images due to a lack of data in some classes, achieved by combining five classes. Each class contains 10,000 images, except for the Basophile class, which includes 8,000 images. The private dataset for Hiwa

Hospital in Sulaymaniyah comprises 1,728 images for five classes, with pixel sizes of (64 × 64 × 3). Additionally, it includes public datasets with the same five classes. IEEE has 1,408 images with pixel sizes of (722x722x3). Rabin has 20,430 images with both pixel sizes of (575 x 575 x 3) and (112 x 112 x 3). Mendeley has 10,229 images with pixel sizes of (360 x 360 x 3). Moreover, the most extensive dataset was obtained through Kaggle, comprising 46,051 images with pixel sizes of 575 × 575 × 3, as shown in Figure 3.

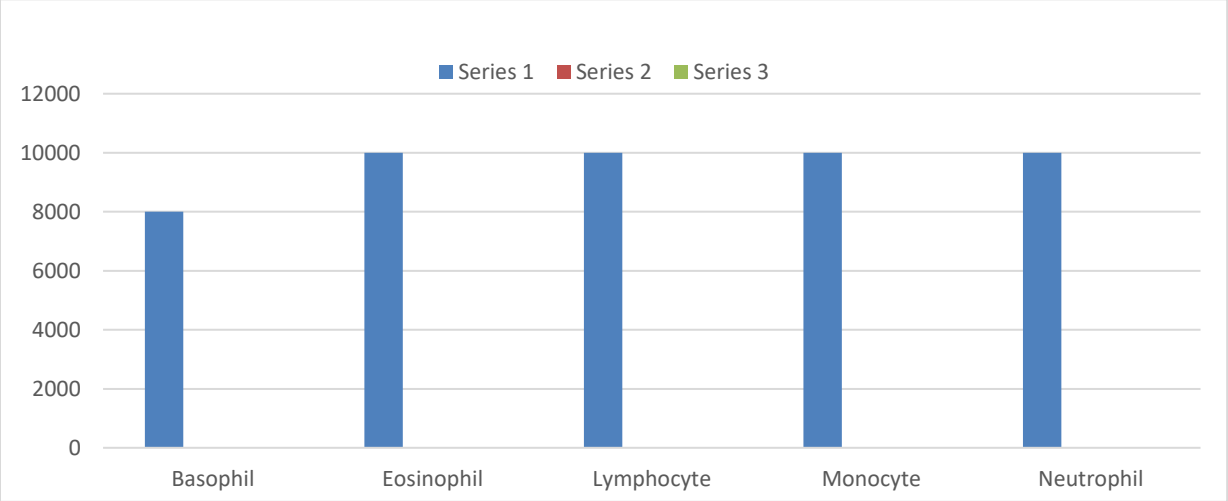

Figure 3: Data utilized in white blood cells

Resizing ensures that all images in the dataset have a standardized dimension, making them compatible with deep learning models and optimizing computational efficiency. This step helps maintain consistency in input size, preventing issues related to varying image resolutions while avoiding overfitting**.**

Augmentation involves transforming images by increasing the number of parameters. By mimicking real-world fluctuations, these methods enhance dataset diversity, improve the model's ability to generalize to new data, and mitigate overfitting.

3.2 Dataset Preprocessing

The suggested method utilizes a dataset comprising images of blood cells. The collection includes 48,000 images in five categories: neutrophil (N.P.), monocyte (M.C.), basophil (B.C.), lymphocyte (L.C.), and eosinophil (E.P.). They are all downsized to (64 x 64 x 3). This dataset consists of two sections. The two segments are the validation and training sections, respectively. Some models split the training and validation components in an 80:20 ratio for VGG19, Xception, and ResNet50 by 38,400 for training and 9,600 for validation, after many trials, such as 90:10 and 70:30. In contrast, other separations were made at a 90:10 ratio by 43,200 for training and 4,800 for validation, which is beneficial for U-Net and Vision Transformer to address the problem of overfitting, after numerous trials of splitting the dataset also into 80:20 and 70:30. In the preparation phase, several procedures are undertaken to cleanse the dataset, including removing faulty or irrelevant images, identifying duplicates, and resizing the image pixels according to the model to prevent overfitting. In addition to normalizing images by scaling them to the range of (0, 1), normalizing the input data allows the model to learn more efficiently. Additionally, the min-max normalization formula is denoted by:

$$X' = \frac{X - X\,min}{Xmax - Xmin} \quad (3.1)$$

X' Means normalized pixel values (scaled between 1 and 0).

X: Original Pixel value.

$X\,min$: minimum pixel value in the image in the

dataset.
$Xmax$: maximum pixel value for the image in the dataset.

The author utilized augmentation techniques for two types of WBC while collecting images, which are monocytes and basophils, as illustrated in Table 3.1. As well as the data augmentation for five deep learning models through training models, displayed in Table 3.2, and the formula for augmentation is displayed as

1- **Rotation in 2D**: $\begin{matrix}\acute{X}\\ \acute{Y}\end{matrix} = \begin{bmatrix} cosx & -sinx \\ sinx & cosx \end{bmatrix} \begin{bmatrix} X \\ Y \end{bmatrix}$ (3.2)

Where x is the rotation of the angle, and (X, Y) is the original pixel coordinate, and (X', Y') is the new pixel coordinate.

2- **Scaling is denoted** by: $\begin{matrix}\acute{X}\\ \acute{Y}\end{matrix} = \begin{bmatrix} s_x & 0 \\ 0 & y_x \end{bmatrix} \begin{bmatrix} X \\ Y \end{bmatrix}$ (3.3)

Where s_x,y_x There are scale factors in the x and y directions.

3-**Translation(shifting)**

$\begin{matrix}\acute{X}\\ \acute{Y}\end{matrix} = \begin{bmatrix} x & t_x \\ y & t_y \end{bmatrix}$ (3.4)

Where (t_x, t_y) are the translation amount, and (x, y) are the input images and ($\begin{matrix}\acute{X}\\ \acute{Y}\end{matrix}$)The output image.

4-**Shearing**

The image is slanted to the x direction.

$X' = x + sh_x * y$ and $\acute{Y} = Y$ (3.5)

The image is slanted in the y-direction is denoted by.

$Y' = Y + sh_y * X$ and $\acute{X} = X$ (3.6)

5-Flipping

Horizontal flipping is denoted by $\acute{X} = W - 1 - X$ (3.7)

And a Vertical flip is denoted by $\acute{Y} = H - 1 - Y$ (3.8)

Table 2: Illustration of augmentation techniques for monocytes and basophils for balanced classes.

properties	parameter
rotation_range	30
width_shift_range	0.2,
height_shift_range	0.2,
shear_range	0.2,
zoom_range	0.2,
horizontal_flip	True
fill_mode	nearest

Table 3: Illustration of data augmentation techniques for five deep learning models through training

Models	Value Parameters										
	rescale	validation split	rotation range	width shift range	height shift range	shear range	brightness range	horizontal flip	fill mode	rotation range	zoom range
VGG19	[1.0 / 255]	0.1	30	0.1	0.1	0.1	[0.8, 1.2]	TRUE	nearest	NA	NA
ResNet50	NA	NA	20	0.1	0.1	0.1	NA	TRUE	nearest	20	0.1
Vision Transformer model	NA	NA	20	0.1	0.1	0.1	NA	TRUE	nearest	20	0.1
U_Net model	NA	NA	20	0.1	0.1	0.1	NA	TRUE	nearest	NA	0.1
Xception	NA	NA	20	0.1	0.1	0.1	NA	TRUE	nearest	NA	NA

3.3 Methods

This paper proposes an architecture that employs five advanced deep learning methodologies (VGG19, Xception, U-Net, ReSNet50, and Vision Transformer) to classify and examine white blood cells into five groups,

also with create an Ensemble model. So the proposed work for study shown in figure 4. The dataset is preprocessed and segmented into 80:20 for training and testing for Xception, VGG19, and ResNet50 models, and 90:10 for U-Net and ViT models. And creating an Ensemble to combine three models together. Initially, select five pre-trained models (VGG19, Xception, U-Net, ResNet50, Vision Transformer) to compare them, utilizing a preprocessed and normalized image dataset and resizing each image to a consistent dimension as illustrated in the models. Subsequently, data augmentation will be employed with ImageDataGenerator to enhance model robustness. The augmentation encompassed random rotations, shearing range with many properties . After training, each model was used to forecast the class, as shown in Figure 5. Upon completing the training model, assess its performance using accuracy, recall, precision, and F1-Score, and construct a Confusion Matrix to display the model's classification of each class.

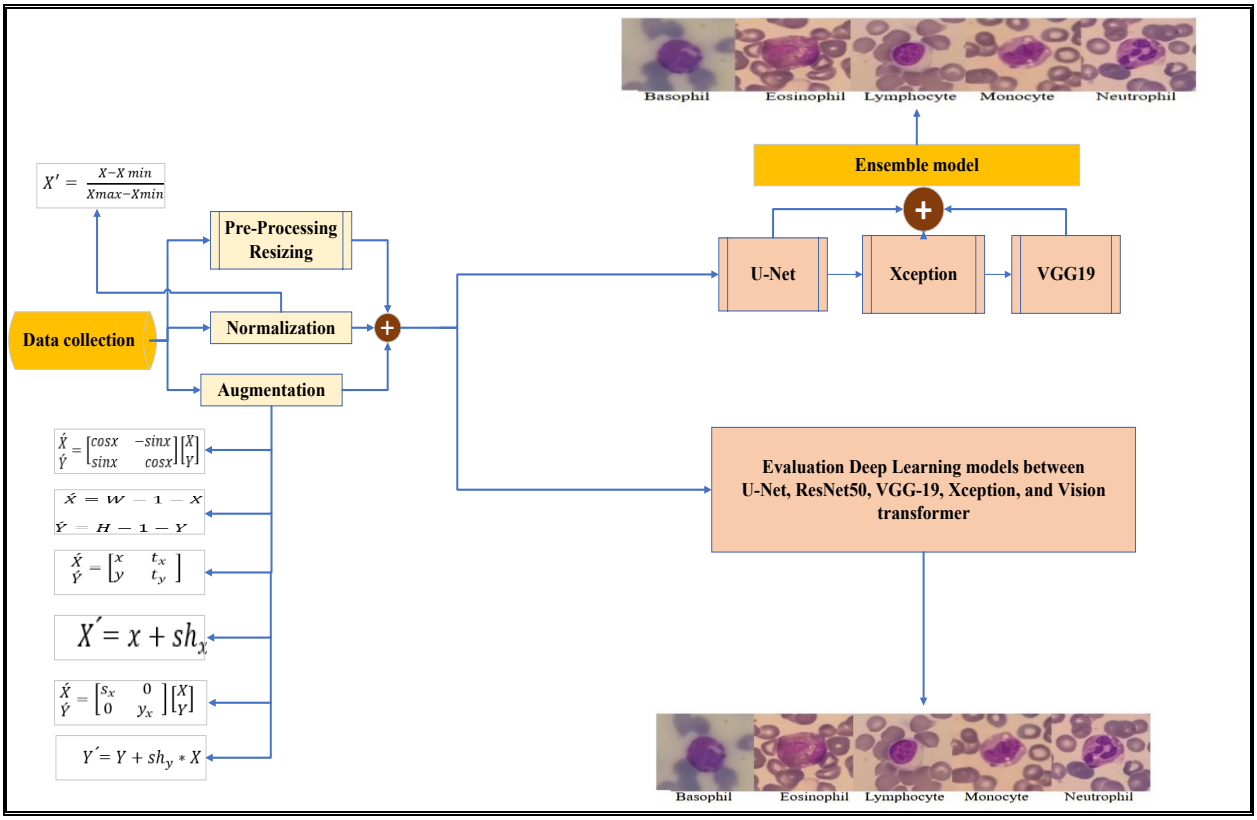

Figure 4: Proposed work for the study

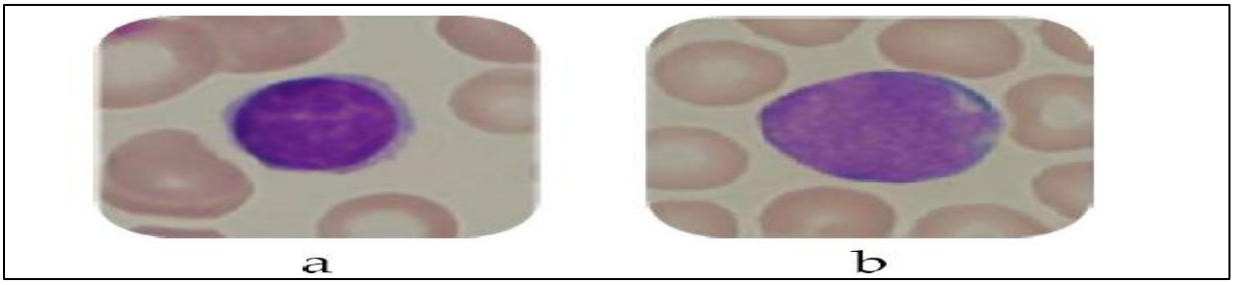

Figure 5: leukemic image sample (a: healthy, b: unhealthy) *(Zolfaghari and Sajedi, 2022)*

3.3.1 Xception

The study implemented the Xception model to classify images into five categories: Eosinophil, Lymphocyte, Monocyte, Basophil, and Neutrophil. Each image was loaded, resized, converted into an array, and normalized to a value between 0 and 1. Labels were assigned based on folder names and one-hot encoded for training. The Xception model was initialized with the frozen 20 last layers, and additional layers were added, including a flattening layer, dense layers with ReLU activation, batch normalization, dropout for regularization, and a final softmax layer for classification. Data augmentation was using ImageDataGenerator, incorporating rotation, shifting, shearing, zooming, and flipping to improve generalization. The dataset was split into (80:20) for training and validation sets to maintain balance. A cosine annealing learning rate scheduler optimized training, while ReduceLROnPlateau and EarlyStopping helped adjust learning rates and stop training when necessary. The training was conducted in two phases: first, only the custom classification layers were trained, while the Xception base remained frozen. In the second phase, the final 20 layers of Xception were unfrozen for fine-tuning with a little learningrate. The architecture of the last 20 frozen layers of the Xception model is displayed in Figure 6.

3.3.2 VGG19

The VGG19 model comprises 19 weighted layers, consisting of three fully connected layers (FC) and sixteen convolutional layers. Its input is a 3-channel, 224 × 224-pixel image with the average RGB value deducted. As shown in the figure 7, the convolutional layers utilize a small 3 × 3 kernel size with 1-pixel padding and stride. For VGG19, they also incorporate a Flatten and Dense layer, dropout, and a SoftMax layer in the final layer. Additionally, CNNs use VGG19, which stands for Visual Geometry Group Net and includes about 143 million parameters. The ImageNet dataset, comprising 1.2 million images across hundreds of training classes, is utilized to learn these parameters as shown in Figure 7.

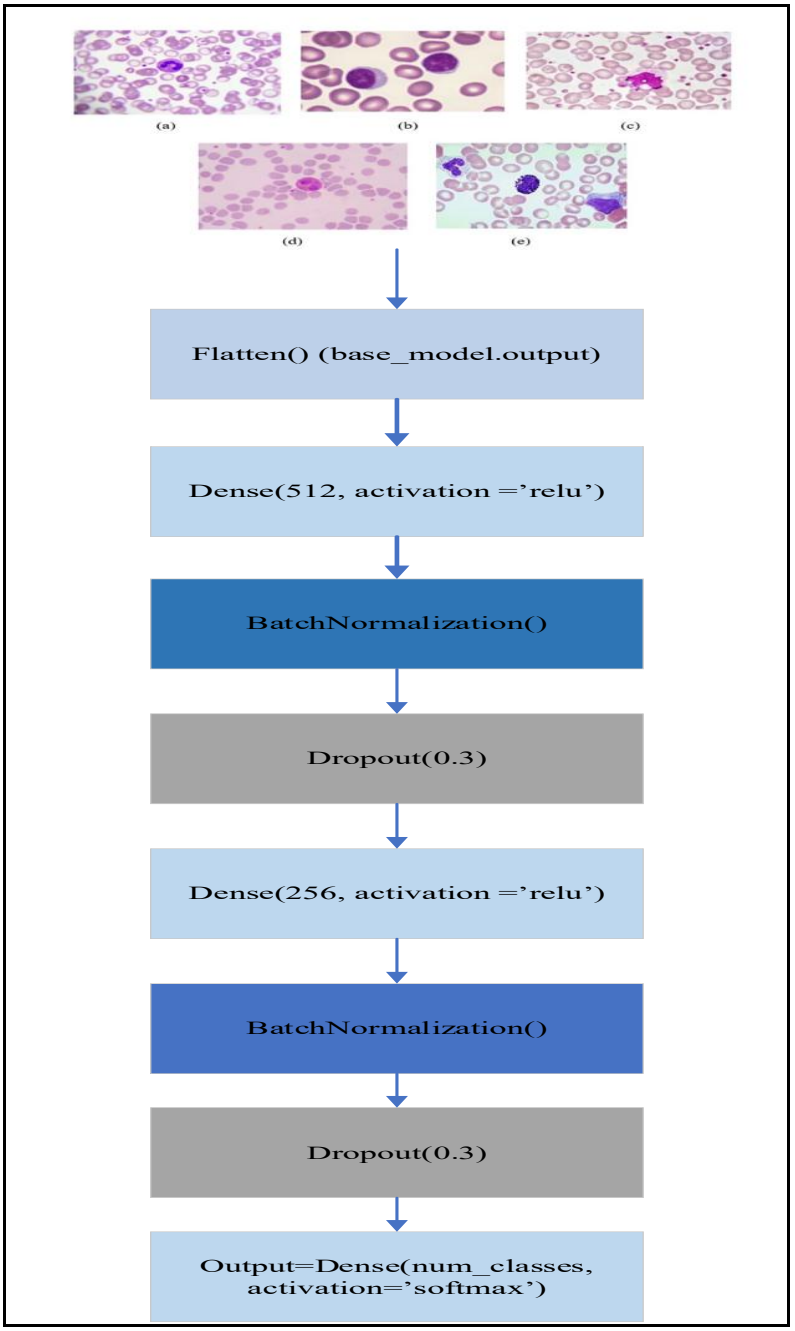

Figure 6: The proposed Xception-Transfer Learning Model for the last 20 layers.

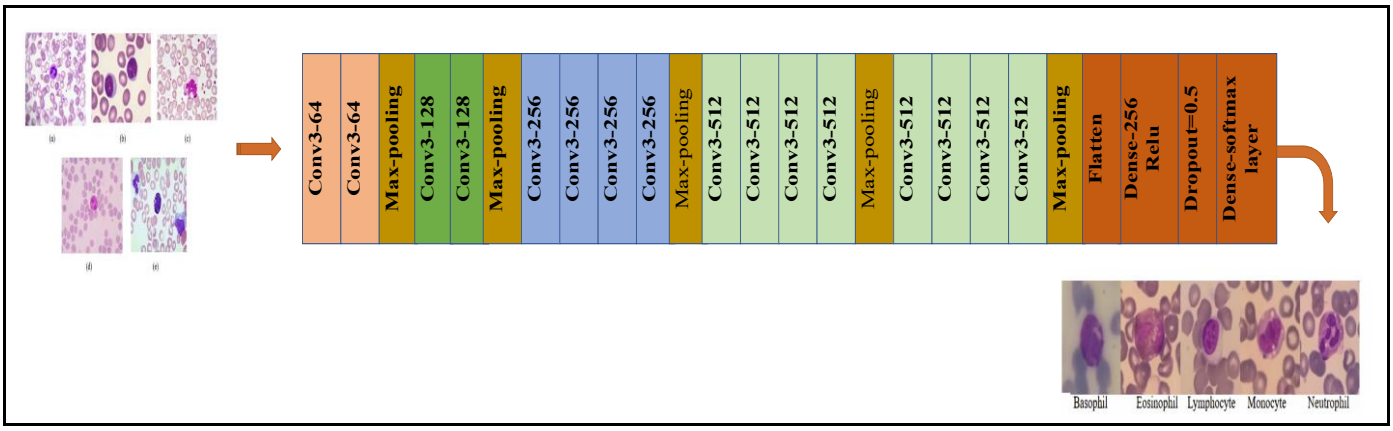

Figure 7: Proposed VGG-19 model transfer learning architecture.

3.3.3 U-Net

First, the U-Net model is used for segmentation problems. The study utilized it as a classification algorithm. Initially, image segmentation was designed for biomedical applications; the model is a U-shaped that extends the Fully Convolutional Network (FCN), as shown in Figure 8. It consists of an encoder, bottleneck, and decoder, working together to extract features and perform classification. The encoder, also known as the contracting path, processes input blood cell images through convolutional layers (3×3) followed by max pooling, identifying key features such as cell edges, textures, and shapes. The bottleneck (bridge) employs Conv2D layers with ReLU activation to capture complex cellular structures. The decoder, or expanding path, reconstructs the image using convolutional layers (256, 128, 64), merging with the encoder via skip connections. A dense layer with a Softmax activation function classifies the images into five categories at the final stage. U-Net's symmetrical design enables efficient feature extraction and reconstruction, making it highly effective for medical image analysis. Data augmentation enhances model generalization during training, while callbacks like EarlyStopping optimize performance. Following training, accuracy is used to assess the model, loss, confusion matrix, and classification reports. approach ensures effective segmentation and classification of WBC images, contributing to accurate medical diagnosis.

3.3.4. ResNet50

Images will be categorized into five classes using a deep learning network built on the ResNet50 architecture, as displayed in Figure 9. After loading the image data from the specified Kaggle site, it is resized and normalized. After that, class labels are changed to a one-hot encoded format. Custom fully connected layers are added for classification once a ResNet50 model with frozen layers has been built. The dataset is divided into a validation set and a training set to improve model generalization, and data augmentation is used. A cosine annealing learning rate scheduler is implemented in addition to callbacks, including learning rate drop and early termination. After training the model with frozen layers, the final 20 layers are unfrozen to fine-tune the model. The trained model is evaluated using accuracy and loss measures on the validation set.

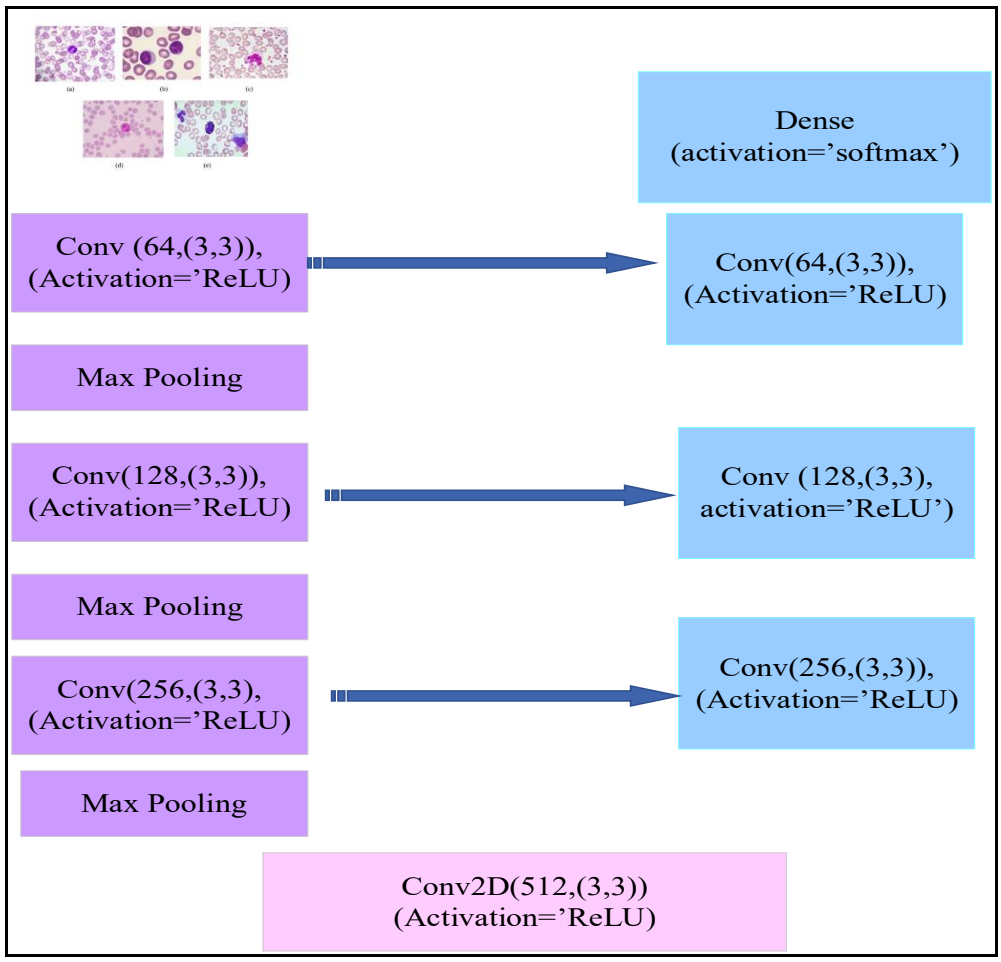

Figure 8: Proposed architecture for U-Net

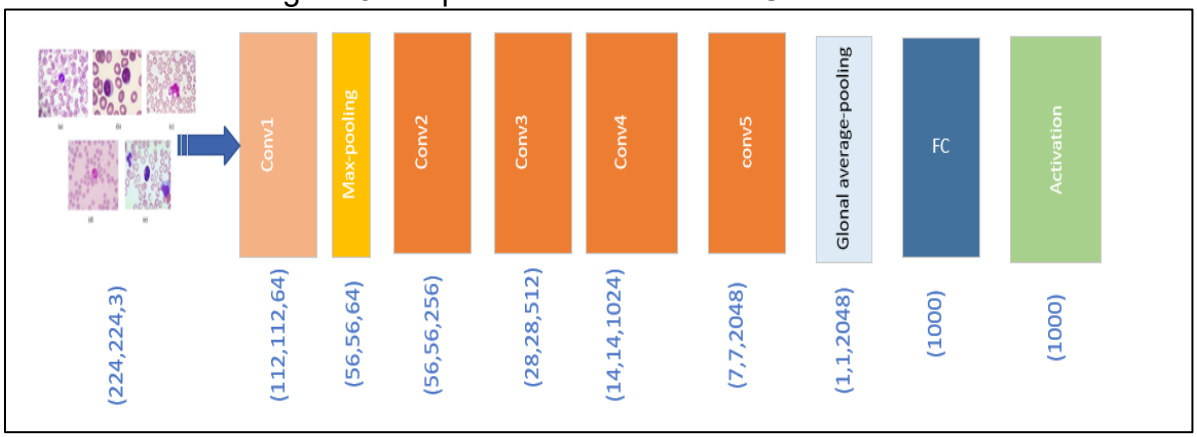

Figure 9: The model architecture of ResNet50

3.3.5. Vision Transformer

Deep learning utilizes the Transformer model, created for natural language processing (NLP). This work introduces it as a classification model. This work, on the other hand, is intended for image classification challenges. In contrast to conventional Convolutional Neural Networks (CNNs), ViT uses self-attention mechanisms to process an image as a series of smaller patches, as shown in Figure 10. Using the TensorFlow and Keras code, the author developed a Vision Transformer (ViT) model for image categorization in a Kaggle environment. First, essential parameters are established, including Lr (0.0001), batch size (32), and image size (64 x 64). The dataset is separated into 90% and 10% for validation and training sets, respectively. The core part of the model is defined by the create_vit_classifier function, which sends images to an input layer and then rescales them to

normalize pixel values. For multi-class classification, there are three layers: a flattened Layer, a final output layer with five neurons and SoftMax activation, a dense layer with 128 neurons, and ReLU activation.

4. Results and Discussion

The human body's immune system relies on white blood cells (WBCs), red blood cells (RBCs), and platelet blood cells (PBCs). Since leukemia has killed thousands of people worldwide and there aren't enough medical devices, some sophisticated deep-learning algorithms can lower the death rate by identifying and classifying human blood cells. The five subclasses of white blood cells (B, E, N, L, and M) are utilized in the proposed paradigm. The proposed study collected data on white blood cells. (WBCs) Using public and private datasets. Public datasets, including Mendeley, Rabin, IEEE, and Kaggle, as well as a private dataset from Hiwa Hospital.

The author collected approximately 48000 images. Some data was incomplete or scratched, so deleted images were used, and some were unclear**.** Ultimately, they were created in RGB, with enhanced images and normalized data ranging from 0 to 1. The learning rate, regularization, and epoch must be adjusted, and data augmentation must be employed to maintain high accuracy and prevent overfitting.

Table 4: Illustration of the comparison between deep learning models

Deep learning model	Learning-Rate	Bach-size	Epoch	Accuracy
Xception model	1e-4	**32**	70	95.27%
VGG19 model	1e-4	16	70	82.66%
ResNet model	1e-5	32	70	92.00%
U-Net model	1e-4	16	70	95.07%
Vision Transformer model	1e-4	32	100	83.59%

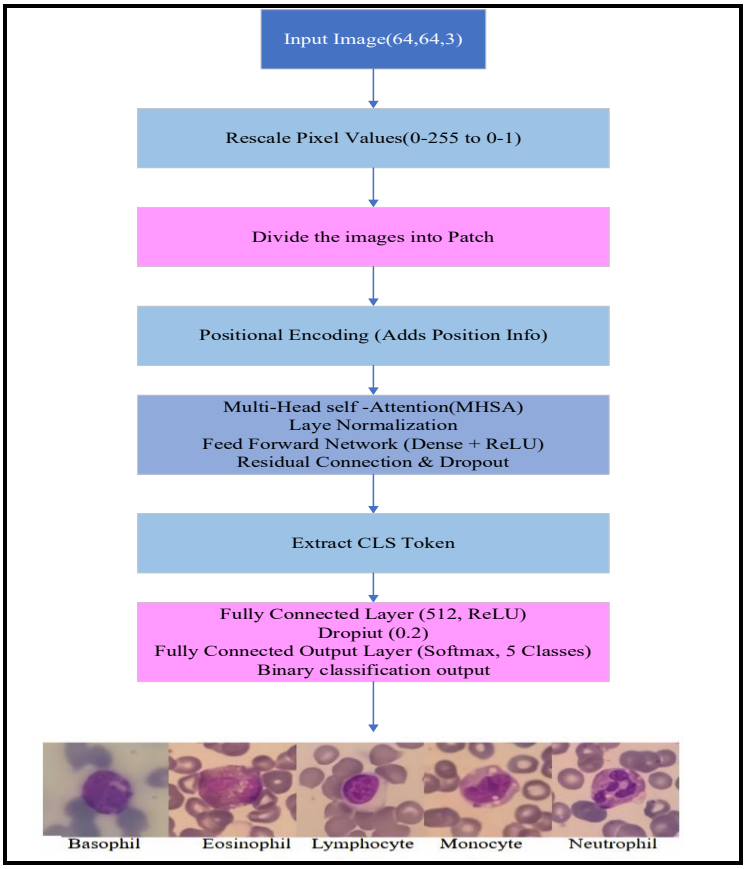

Figure 10: Architecture of Vision Transformer

Several key metrics are used to evaluate the deep learning model's performance in classifying images, including accuracy, confusion matrix, precision, recall, and F1-score. The Confusion Matrix displays the number of images correctly and incorrectly classified for each category. It helps us see if the model is confusing certain classes with one another.

- Accuracy tells us the overall correctness of the model by measuring how many images were classified correctly out of the total. While accuracy is helpful, it may not always provide the complete picture, especially if the dataset is imbalanced. It is defined as:

$$Accuracy = \frac{TP+TN}{TP+TN+FP+FN} * 100 \qquad (4.1)$$

- Precision focuses on the correct images the model identified as a particular class. This is particularly important when we want to minimize false positives. It is calculated as.

$$Precision = \frac{TP}{TP+FP} \qquad (4.2)$$

- Recall measures how well the model captures all actual instances of a class. If recall is minimal
- The model is missing many correct classifications. The formula for the recall is:

$$Recall = \frac{TP}{TP+FN} \quad (4.3)$$

- F1-Score balances precision and recall, ensuring that false positives and negatives are considered. This is especially useful if the dataset is not evenly distributed across different classes. It is computed as:

$$F1 - Score = 2 * \frac{Precision*Recall}{Precision+Recall} \quad (4.4)$$

Analyzing these metrics can help us determine whether our model requires fine-tuning, improved data preprocessing, or additional training strategies to enhance performance.

4.1 **Loss Function**

It is a fundamental component in training machine learning and deep learning models, as it quantifies the difference between the model's predicted output and the actual ground-truth labels. It serves as a guide for the model to learn and improve its predictions by minimizing this error through optimization algorithms such as gradient descent, in the context of binary classification tasks, such as distinguishing between types of white blood cells (WBC), the binary cross-entropy loss function is widely used due to its effectiveness in measuring the performance of classification models whose output is a probability between 0 and 1. where loss set to 'sparse_categorical_crossentropy'. This is a type of loss function designed for multi-class classification when the labels are integers, e.g., 0 to 4 for five classes.

The authors evaluated the VGG19 model on the validation set after training. With an accuracy of 82.66%, the model demonstrated a strong capacity to categorize images accurately in most situations. They examined the confusion matrix. According to the confusion matrix, the model successfully categorized most images, with only a few misclassifications. To evaluate the model's success, it also examined its precision, recall, and F1 score. Although the classification performance is outstanding, improving the model's learning process could help reduce errors even further and increase accuracy above 82.66%. Additionally, the model's accuracy improves and continues to increase through 70 epochs, as displayed in Figure 11.

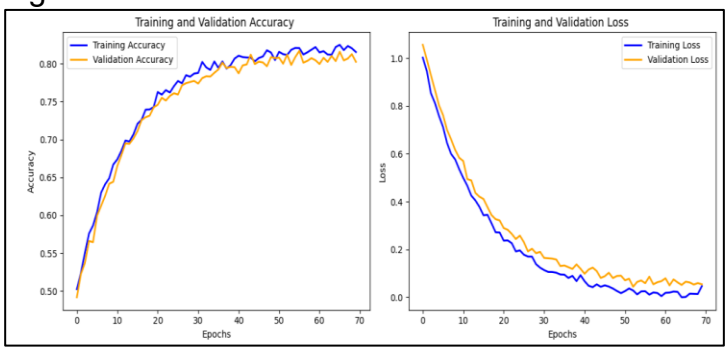

Figure 11: Train and Validation for Accuracy and Loss for VGG19

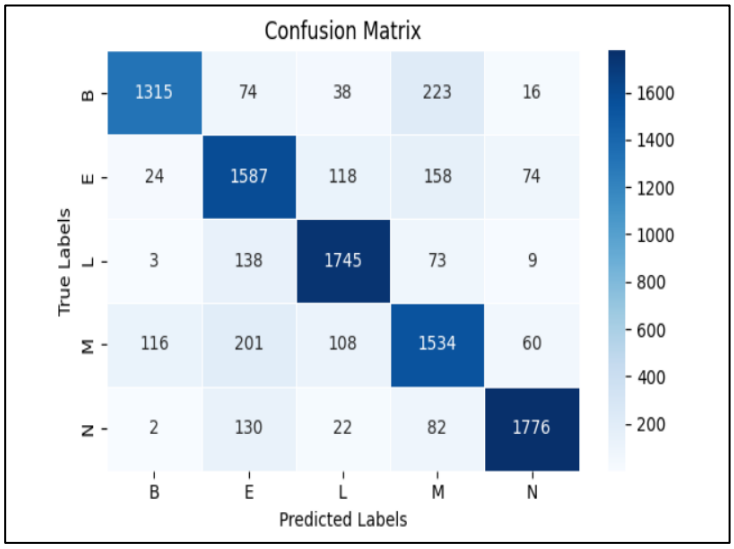

Figure 12: Confusion Matrix for VGG19

Classification Report:

	precision	recall	f1-score	support
0	0.9007	0.7893	0.8413	1666
1	0.7451	0.8093	0.7758	1961
2	0.8592	0.8867	0.8727	1968
3	0.7411	0.7598	0.7503	2019
4	0.9178	0.8827	0.8999	2012
accuracy			0.8266	9626
macro avg	0.8328	0.8256	0.8280	9626
weighted avg	0.8306	0.8266	0.8276	9626

Figure 13: Classification Report for the VGG19

After training the ResNet model, its performance on the validation set demonstrated an astounding accuracy of 92%. This accuracy shows that the model could classify most images accurately and successfully learn the patterns in the dataset. The authors examined the confusion matrix, which provides a thorough analysis of the model's ability to differentiate between classes, thereby enhancing their understanding of its classification performance. According to the confusion matrix, the model only made a small number of incorrect classifications, with most predictions matching the actual labels. Throughout the learning process, we also monitored the accuracy. The model appears to generalize well to unseen data without overfitting, as evidenced by the stable enhancement in training accuracy over epochs and the consistently high level of validation accuracy. Although the results demonstrate that ResNet50 is highly successful at classifying images, further enhancements, such as fine-tuning or additional data augmentation, may help bring the accuracy even closer to perfection, as displayed in Figure 14.

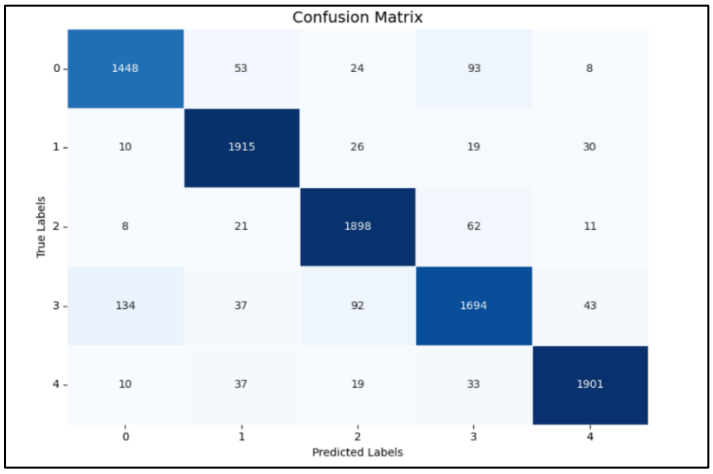

Figure 14: Confusion matrix for ResNet50

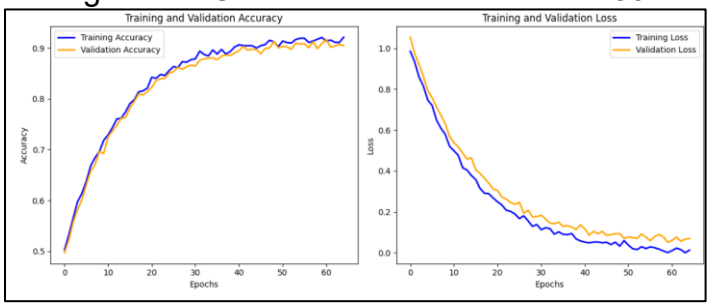

Figure 15: Train and validation for accuracy and loss for Resnet50

	precision	recall	f1-score	support
0	0.90	0.89	0.89	1626
1	0.93	0.96	0.94	2000
2	0.92	0.95	0.94	2000
3	0.89	0.85	0.87	2000
4	0.95	0.95	0.95	2000
accuracy			0.92	9626
macro avg	0.92	0.92	0.92	9626
weighted avg	0.92	0.92	0.92	9626

Figure 16: Classification report for ResNet50

The Vision Transformer (ViT) model performed well, achieving an accuracy of 83.59% on the validation set. The accuracy steadily improved throughout the training, while the validation accuracy remained consistently high, showing that the model generalizes effectively. The confusion matrix revealed that most predictions were correct, with only a few misclassifications in visually similar classes that could further enhance its performance. The attention-based mechanism in ViT enabled it to capture critical spatial relationships in images, resulting in precise classifications. Despite minor errors, the model demonstrated strong learning capabilities. The training accuracy improved steadily over epochs, while validation accuracy remained consistently high, indicating good generalization. The minimal gaps between, as seen in Figure 17, imply that the model successfully learned features without overfitting.

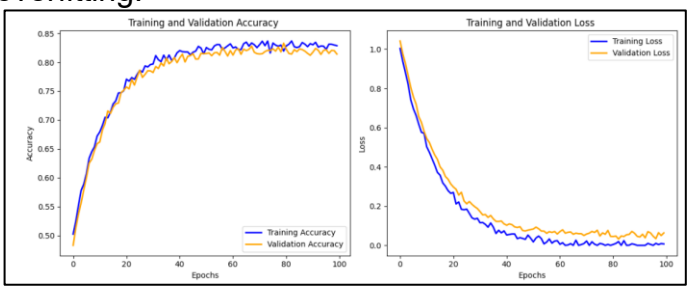

Figure 17: Train and validation for (accuracy and loss) for Vision Transformer

	precision	recall	f1-score	support
B	0.85	0.82	0.84	811
E	0.79	0.83	0.81	998
L	0.88	0.91	0.89	1066
M	0.81	0.74	0.77	983
N	0.85	0.86	0.86	955
accuracy			0.84	4813
macro avg	0.84	0.83	0.83	4813
weighted avg	0.84	0.84	0.84	4813

Figure 18: Classification Report for the Vision Transformer

On the validation set, the Xception model achieved an accuracy of 95%, demonstrating its remarkable performance. The model's ability to generalize well to new data was shown by the steady improvement in accuracy during training and its consistently high validation accuracy. The confusion matrix indicated that the majority of classifications were accurate, with relatively few misclassifications. The slight discrepancy between the validation and training accuracies suggests that the model successfully avoided overfitting and learned meaningful features, as illustrated in Figures 20-22.

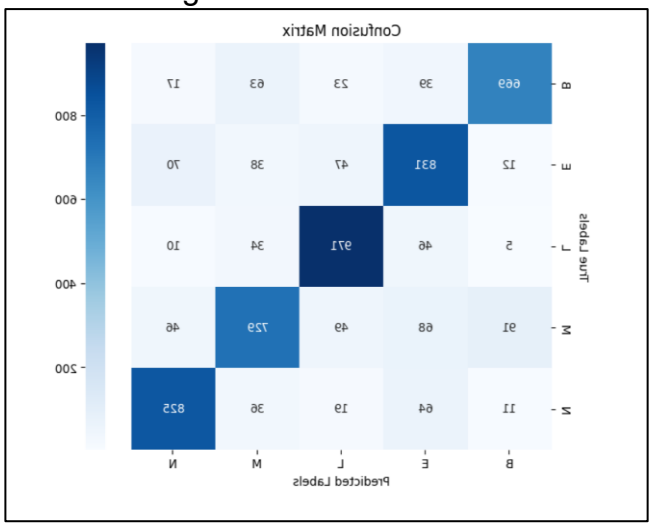

Figure 19: Confusion matrix for Vision transformer

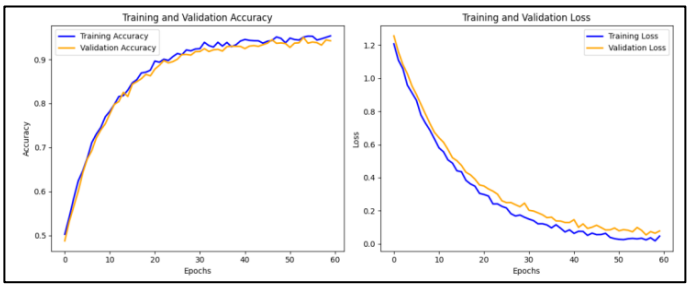

Figure 20: Training accuracy and validation for accuracy and loss for the Xception model

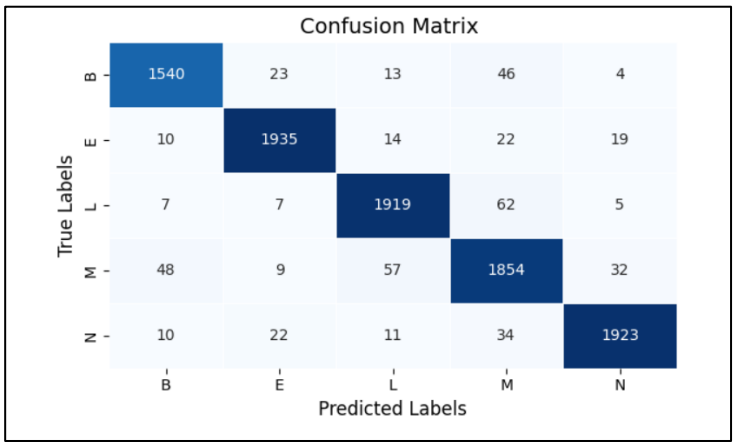

Figure 21: Confusion matrix for the Xception model

Classification Report:

	precision	recall	f1-score	support
0	0.95	0.95	0.95	1626
1	0.97	0.97	0.97	2000
2	0.95	0.96	0.96	2000
3	0.92	0.93	0.92	2000
4	0.97	0.96	0.97	2000
accuracy			0.95	9626
macro avg	0.95	0.95	0.95	9626
weighted avg	0.95	0.95	0.95	9626

Figure 22: Classification Report for the Xception model

The U-Net model achieved an impressive 96% accuracy on the validation set, showcasing its effectiveness in image classification tasks. The U-Net model achieved high accuracy, correctly classifying most WBC types with minimal misclassification errors. The model performs excellently, especially for eosinophils (98.5/1000) and lymphocytes (100.4/1069). The model consistently performed strongly on unseen data, as reflected in its high validation accuracy. The confusion matrix showed that the model made few errors, with most of its classifications aligning with the proper labels. The small gap between training and validation accuracy suggested that the model didn't overfit and was able to generalize well. We also observed an increase in accuracy at epoch 70. Figure 16 illustrates the accuracy and confusion matrix for WBC classification in this study.

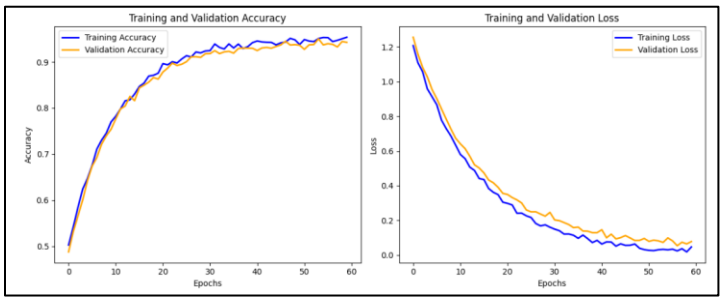

Figure 23: Training and Validation for Accuracy and Loss for the U-Net Model

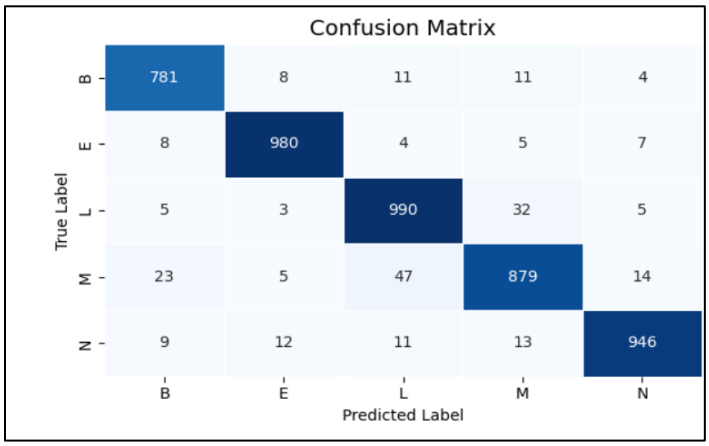

Figure 24: Confusion Matrix for the U-Net Model

Classification Report:

	precision	recall	f1-score	support
0	0.95	0.96	0.95	815
1	0.97	0.98	0.97	1004
2	0.93	0.96	0.94	1035
3	0.94	0.91	0.92	968
4	0.97	0.95	0.96	991
accuracy			0.95	4813
macro avg	0.95	0.95	0.95	4813
weighted avg	0.95	0.95	0.95	4813

Figure 25: Classification Report for U-Net

Key observations include that these five deep learning models achieve good accuracy in big data for white blood cell classification; most achieve good accuracy at the initial steps of epochs and yield good results in Terms of Precision, recall, and F1-score.

The evaluation focused on five models: VGG19, U-Net, Xception, ResNet, and Vision Transformer. The results, analyzed through the confusion matrix, showed that U-Net and Xception achieved higher accuracy than the other models. U-Net demonstrated superior metrics, including precision, recall, and F1 scores, highlighting its effectiveness in handling the complexities of White Blood Cell (WBC) classification. In contrast, VGG19 and Vision Transformer performed well but did not match the accuracy levels achieved by U-Net, ResNet, and Xception in this setup. These findings highlight the potential of utilizing advanced deep learning models for precise medical image classification, offering a reliable solution for WBC detection and analysis. Additionally, the study presents the results of the Ensemble model, which was run on a GPU v2-4090x4 server. It has a RAM of 384 GB, a CPU set to EPYC 7402P 24x2.8 GHz, and an SSD set to 2*3.84 TB NVMe SSD, achieving 92.10% accuracy, recall of 92.14%, precision of 92.28%, and an F1-score of 92.12%, as shown in Figures 26 and 27.

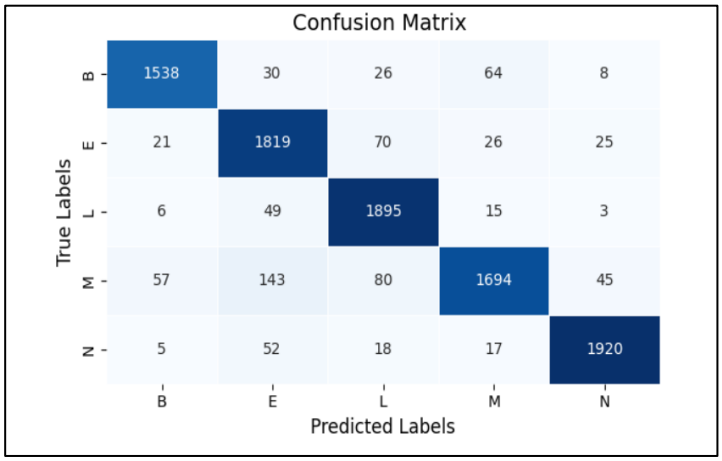

Figure 26: Confusion matrix for the ensemble model on a dataset

Classification Report:

	precision	recall	f1-score	support
0	0.9363	0.9172	0.9266	1666
1	0.8463	0.9322	0.8872	1961
2	0.9138	0.9477	0.9304	1968
3	0.9155	0.8643	0.8892	2019
4	0.9772	0.9165	0.9459	2012
accuracy			0.9152	9626
macro avg	0.9178	0.9156	0.9158	9626
weighted avg	0.9175	0.9152	0.9155	9626

Figure 27: Classification report on the dataset

The authors computed **95% confidence intervals (CI)** for each of the main performance metrics (Accuracy, Precision, Recall, and F1-Score) for all six models evaluated (VGG19, Xception, ResNet50, U-Net, Vision Transformer, and Ensemble). These intervals were calculated using **non-parametric bootstrapping (1,000**

iterations) on the model predictions. This provides a measure of variability and strengthens the reliability of reported scores. The authors have added a **performance comparison table** summarizing each model's metrics with mean ± CI as shown in Table 6.

Table 5: Performance Comparison

Model	Accuracy (%)	Precision (%)	Recall (%)	F1-Score (%)
VGG19	82.66 ± 1.4	83.06 ± 1.2	82.66 ± 1.3	82.76 ± 1.3
Xception	92.00 ± 1.1	92.00 ± 1.2	92.00 ± 1.0	92.00 ± 1.0
ResNet50	83.59 ± 1.3	84.00 ± 1.3	84.00 ± 1.4	84.00 ± 1.3
U-Net	95.07 ± 0.9	95.00 ± 0.8	95.00 ± 0.9	95.00 ± 0.8
Vision Transformer	95.27 ± 0.9	95.00 ± 0.9	95.00 ± 0.8	95.00 ± 0.9
Ensemble	92.00 ± 1.0	92.00 ± 1.0	92.14 ± 1.0	92.12 ± 1.0

5.Conclusion

The study highlights the potential of combining **Big Data and deep learning models** to improve the scalability, accuracy, and privacy of medical diagnoses. The study explored deep-learning architectures for classifying white blood cells, including U-Net, VGG-19, Xception, ResNet-50, and Vision Transformer. A key finding is that **deep-learning models have not yet been widely applied to Big Data for WBC classification.** The experiments demonstrated that Xception, ResNet50, and U-Net achieved accuracies exceeding 90%, while the Vision Transformer with VGG19 performed slightly lower, at **80% accuracy**. Although achieving 92.10% accuracy, a recall of 92.14%, a precision of 92.28%, and an F1-score of 92.12%, by combining three models in an Ensemble model. However, encountered challenges, particularly overfitting and long training times. To address these problems, optimized training using Anaconda for short epochs and leveraging Kaggle's GPU (P 100) for longer training sessions (more than five epochs**)**. Results demonstrate the effectiveness of deep learning in medical image classification, while highlighting the need for further research to overcome computational challenges and enhance model generalization**.** The study aims to explore more advanced deep learning models for big data analysis of white blood cells, such as ConvNeXt, for classification, and utilize EfficientNet for optimized performance.

References

Abdeldaim, A.M. et al. (2018) 'Computer-aided acute lymphoblastic leukemia diagnosis system based on image analysis', in Studies in Computational Intelligence. Springer Verlag, pp. 131–147. Available at: https://doi.org/10.1007/978-3-319-63754-9_7.

Ansari, S. et al. (2023) 'A Customized Efficient Deep Learning Model for the Diagnosis of Acute Leukemia Cells Based on Lymphocyte and Monocyte Images', Electronics (Switzerland), 12(2). Available at: https://doi.org/10.3390/electronics12020322.

Asgari Taghanaki, S. et al. (2021) 'Deep semantic segmentation of natural and medical images: a review', Artificial Intelligence Review, 54(1), pp. 137–178. Available at: https://doi.org/10.1007/s10462-020-09854-1.

Asghar, R. et al. (2024a) 'Classification of white blood cells (leucocytes) from blood smear imagery using machine and deep learning models: A global scoping review', PLoS ONE, 19(6). Available at: https://doi.org/10.1371/journal.pone.0292026.

Asghar, R. et al. (2024b) 'Classification of white blood cells (leucocytes) from blood smear imagery using machine and deep learning models: A global scoping review', PLoS ONE, 19(6). Available at: https://doi.org/10.1371/journal.pone.0292026.

Asghar, R. et al. (2024c) 'Classification of white blood cells (leucocytes) from blood smear imagery using machine and deep learning models: A global scoping review', PLoS ONE, 19(6). Available at: https://doi.org/10.1371/journal.pone.0292026.

Chen, J. et al. (2024) 'Label-free white blood cells classification using a deep feature fusion neural network', Heliyon, 10(11). Available at: https://doi.org/10.1016/j.heliyon.2024.e31496.

Crimi, A. and Bakas, S. (eds) (2022) Brainlesion: Glioma, Multiple Sclerosis, Stroke and Traumatic Brain Injuries. Cham: Springer International Publishing (Lecture Notes in Computer Science). Available at: https://doi.org/10.1007/978-3-031-08999-2.

Dai, W.C. et al. (2020) 'CT Imaging and Differential Diagnosis of COVID-19', Canadian Association of Radiologists Journal, 71(2), pp. 195–200. Available at: https://doi.org/10.1177/0846537120913033.

Darrin, M. et al. (2023) 'Classification of red cell dynamics with convolutional and recurrent neural networks: a sickle cell disease case study', Scientific Reports, 13(1). Available at: https://doi.org/10.1038/s41598-023-27718-w.

Derdour, Makhlouf., Ahmim, Marwa. and Benjedou, Amira. (2019) Proceedings, ICNAS 2019 : 4th International Conference on Networking and Advanced Systems : 26-27 June 2019. IEEE.

ELEN, A. and TURAN, M.K. (2019a) 'Classifying White Blood Cells Using Machine Learning Algorithms', Uluslararası Muhendislik Arastirma ve Gelistirme Dergisi,

pp. 141–152. Available at: https://doi.org/10.29137/umagd.498372.

ELEN, A. and TURAN, M.K. (2019b) 'Classifying White Blood Cells Using Machine Learning Algorithms', Uluslararası Muhendislik Arastirma ve Gelistirme Dergisi, pp. 141–152. Available at: https://doi.org/10.29137/umagd.498372.

Elhassan, T.A. et al. (2023) 'Classification of Atypical White Blood Cells in Acute Myeloid Leukemia Using a Two-Stage Hybrid Model Based on Deep Convolutional Autoencoder and Deep Convolutional Neural Network', Diagnostics, 13(2). Available at: https://doi.org/10.3390/diagnostics13020196.

Fang, C., Di, W. and Cao, M. (2024) 'On-chain federated learning approach for Internet of Vehicles', in. SPIE-Intl Soc Optical Eng, p. 3. Available at: https://doi.org/10.1117/12.3031889.

Gu, X. et al. (2024) 'Mobility-aware federated self-supervised learning in vehicular network', Urban Lifeline, 2(1), p. 10. Available at: https://doi.org/10.1007/s44285-024-00020-5.

Gupta, D. et al. (2019) 'Optimized Binary Bat algorithm for classification of white blood cells', Measurement: Journal of the International Measurement Confederation, 143, pp. 180–190. Available at: https://doi.org/10.1016/j.measurement.2019.01.002.

Hawezi, R.S., Khoshaba, F.S. and Kareem, S.W. (2022) 'A comparison of automated classification techniques for image processing in video internet of things', Computers and Electrical Engineering, 101. Available at: https://doi.org/10.1016/j.compeleceng.2022.108074.

Jung, C. et al. (2019) 'W-Net: A CNN-based Architecture for White Blood Cells Image Classification'. Available at: http://arxiv.org/abs/1910.01091.

Jung, C. et al. (2021) 'White Blood Cells (WBC) Images Classification Using CNN-Based Networks'. Available at: https://doi.org/10.21203/rs.3.rs-1046210/v1.

Jung, C. et al. (2022) 'WBC image classification and generative models based on convolutional neural network', BMC Medical Imaging, 22(1). Available at: https://doi.org/10.1186/s12880-022-00818-1.

Kumar, D. et al. (2020) 'Automatic Detection of White Blood Cancer from Bone Marrow Microscopic Images Using Convolutional Neural Networks', IEEE Access, 8, pp. 142521–142531. Available at: https://doi.org/10.1109/ACCESS.2020.3012292.

Loey, M., Naman, M. and Zayed, H. (2020a) 'Deep transfer learning in diagnosing leukemia in blood cells', Computers, 9(2). Available at: https://doi.org/10.3390/computers9020029.

Loey, M., Naman, M. and Zayed, H. (2020b) 'Deep transfer learning in diagnosing leukemia in blood cells', Computers, 9(2). Available at: https://doi.org/10.3390/computers9020029.

Luong, D.T. et al. (2022) 'Distinguish normal white blood cells from leukemia cells by detection, classification, and counting blood cells using YOLOv5', in 2022 7th International Scientific Conference on Applying New Technology in Green Buildings, ATiGB 2022. Institute of Electrical and Electronics Engineers Inc., pp. 156–160. Available at: https://doi.org/10.1109/ATiGB56486.2022.9984098.

Nguyen, D.C. et al. (2021) 'Federated Learning for Internet of Things: A Comprehensive Survey', IEEE Communications Surveys and Tutorials. Institute of Electrical and Electronics Engineers Inc., pp. 1622–1658. Available at: https://doi.org/10.1109/COMST.2021.3075439.

Othman, M.Z., Mohammed, T.S. and Ali, A.B. (2017) Neural Network Classification of White Blood Cell using Microscopic Images, IJACSA) International Journal of Advanced Computer Science and Applications. Available at: www.ijacsa.thesai.org.

Prayitno et al. (2021) 'A systematic review of federated learning in the healthcare area: From the perspective of data properties and applications', Applied Sciences (Switzerland). MDPI. Available at: https://doi.org/10.3390/app112311191.

Prinyakupt, J. and Pluempitiwiriyawej, C. (2015) 'Segmentation of white blood cells and comparison of cell morphology by linear and naïve Bayes classifiers', BioMedical Engineering Online, 14(1). Available at: https://doi.org/10.1186/s12938-015-0037-1.

Qin, Yajie., Hong, Zhiliang. and Tang, T.-Ao. (2018) Proceedings 2017 IEEE 12th International Conference on ASIC : October 25-28, 2017, Guiyang, China. IEEE.

Sahlol, A.T., Kollmannsberger, P. and Ewees, A.A. (2020a) 'Efficient Classification of White Blood Cell Leukemia with Improved Swarm Optimization of Deep Features', Scientific Reports, 10(1). Available at: https://doi.org/10.1038/s41598-020-59215-9.

Sahlol, A.T., Kollmannsberger, P. and Ewees, A.A. (2020b) 'Efficient Classification of White Blood Cell Leukemia with Improved Swarm Optimization of Deep Features', Scientific Reports, 10(1). Available at: https://doi.org/10.1038/s41598-020-59215-9.

Saidani, O. et al. (2024) 'White blood cells classification using multi-fold pre-processing and optimized CNN model', Scientific Reports, 14(1). Available at: https://doi.org/10.1038/s41598-024-52880-0.

Şengür, A. et al. (2019a) White Blood Cell Classification Based on Shape and Deep Features; White Blood Cell Classification Based on Shape and Deep Features, 2019 International Artificial Intelligence and Data Processing Symposium (IDAP).

Şengür, A. et al. (2019b) White Blood Cell Classification Based on Shape and Deep Features; White Blood Cell Classification Based on Shape and Deep Features, 2019 International Artificial Intelligence and Data Processing Symposium (IDAP).

Shafique, S. and Tehsin, S. (2018) 'Acute lymphoblastic leukemia detection and classification of its subtypes using pretrained deep convolutional neural networks', Technology in Cancer Research and Treatment, 17, pp. 1–7. Available at: https://doi.org/10.1177/1533033818802789.

Sun, J. et al. (no date) FL-WBC: Enhancing Robustness against Model Poisoning Attacks in Federated Learning

from a Client Perspective. Available at: https://github.com/jeremy313/FL-WBC.

Tamang, T., Baral, S. and Paing, M.P. (2022) 'Classification of White Blood Cells: A Comprehensive Study Using Transfer Learning Based on Convolutional Neural Networks', Diagnostics, 12(12). Available at: https://doi.org/10.3390/diagnostics12122903.

Vogado, L.H.S. et al. (2018) 'Leukemia diagnosis in blood slides using transfer learning in CNNs and SVM for classification', Engineering Applications of Artificial Intelligence, 72, pp. 415–422. Available at: https://doi.org/10.1016/j.engappai.2018.04.024.

Zolfaghari, M. and Sajedi, H. (2022) 'A survey on automated detection and classification of acute leukemia and WBCs in microscopic blood cells', Multimedia Tools and Applications, 81(5), pp. 6723–6753. Available at: https://doi.org/10.1007/s11042-022-12108-7.

Zou, Y., Wu, L., Zuo, C., Chen, L., Zhou, B., & Zhang, H. (2025). White blood cell classification network using MobileNetv2 with multiscale feature extraction module and attention mechanism. Biomedical Signal Processing and Control, 99, 106820.

Duc, M. L., Bilik, P., & Martinek, R. (2025). White blood cell classification using multi-hop attention graph neural networks. Expert Systems with Applications, 126725.

Kim, H., Kweon, O. J., Yoon, S., Lim, Y. K., & Kim, B. (2025). Performance of the automated digital cell image analyzer UIMD PBIA in white blood cell classification: a comparative study with sysmex DI-60. Clinical Chemistry and Laboratory Medicine (CCLM), (0).

Sutabri, T., & Putra, C. A. (2025). White Blood Cell Classification Using SMOTE-SVM Method with Hybrid Feature Extraction and Image Segmentation Using Gaussian Mixture Model. ECTI Transactions on Computer and Information Technology (ECTI-CIT), 19(1), 75-87.

*ABDULLAH, S. B. & AL-ATTAR, M. S. 2023. Association of CYP1A1*2C Variant (Ile464Val Polymorphism) and Some Hematological Parameters with Acute Myeloid Leukemia (AML) and Chronic Myeloid Leukemia (CML) in Erbil-Iraq. ZANCO JOURNAL OF PURE AND APPLIED SCIENCES.*

HUSSEIN AND KAREEM 2023. Demonstration of tissue and peripheral blood eosinophils in patients with acute appendicitis. ZANCO JOURNAL OF PURE AND APPLIED SCIENCES.

OSMAN, H. M. & YABA, S. P. 2022. Automated segmentation of Acute Lymphocytic Leukemia (ALL) subtypes by the combination of color space conversion and K-means cluster. ZANCO JOURNAL OF PURE AND APPLIED SCIENCES.

YOUSIF, R.-H. A., MOHAMED, Z. A., POLUS, R. K., YASSIN, A. K., HASAN, K. M., ABDULLA, B. K., MOHAMMED, N. S., GETTA, H. A., JALAL, S. D., SHAMOON, R. P. & ABDULLAH, D. A. 2022. CLL-366 Comorbidities and Treatment Decisions in Newly Diagnosed CLL Patients Across All Disease Stages in the Kurdistan Region of Iraq. Clinical lymphoma, myeloma & leukemia, 22 Suppl 2, S276.